The Astrophysical Journal, 604:495–507, 2004 April 1

THE COSMIC EVOLUTION OF QUASAR HOST GALAXIES

Renato Falomo
INAF–Osservatorio Astronomico di Padova, Vicolo dell'Osservatorio 5, 35122 Padua, Italy; falomo@pd.astro.it

Jari K. Kotilainen
Tuorla Observatory, University of Turku, Väisäläntie 20, FIN-21500 Piikkiö, Finland; jarkot@astro.utu.fi

Claudio Pagani
Università dell'Insubria, via Valleggio 11, 22100 Como, Italy; pagani@mib.infn.it

Riccardo Scarpa
European Southern Observatory, 3107 Alonso de Cordova, Santiago, Chile; rscarpa@eso.org

and

Aldo Treves
Università dell'Insubria, via Valleggio 11, 22100 Como, Italy; treves@mib.infn.it
Received 2003 July 16; accepted 2003 December 9

ABSTRACT

We present the results of a near-infrared imaging study of the host galaxies of 17 quasars in the redshift range $1 < z < 2$. The observations were carried out at the ESO VLT UT1 8 m telescope under excellent seeing conditions ($\sim 0\farcs4$). The sample includes radio-loud (RLQs) and radio-quiet (RQQs) quasars with similar distribution of redshift and optical luminosity. For all the observed objects but one we have been able to derive the global properties of the surrounding nebulosity. The host galaxies of both types of quasars appear to follow the expected trend in luminosity of massive ellipticals undergoing simple passive evolution. However, we find a systematic difference by a factor ~ 2 in the host luminosity between RLQs and RQQs [$\langle M_K \rangle_{\rm RLQ}({\rm host}) = -27.55 \pm 0.12$ and $\langle M_K \rangle_{\rm RLQ}({\rm host}) = -26.83 \pm 0.25$]. Comparison with other samples of quasar hosts at similar and lower redshift indicates that the difference in the host luminosity between RLQs and RQQs remains the same from $z = 2$ to the present epoch. No significant correlation is found between the nuclear and the host luminosities. Assuming that the host luminosity is proportional to the black hole mass, as observed in nearby massive spheroids, these quasars emit at very different levels (spread ~ 1.5 dex) with respect to their Eddington luminosity and with the same distribution for RLQs and RQQs. Apart from a factor of ~ 2 difference in luminosity, the hosts of RLQs and RQQs of comparable nuclear luminosity appear to follow the same cosmic evolution as massive inactive spheroids. Taken together, our results support a view where nuclear activity can occur in all luminous ellipticals without producing a significant change in their global properties and evolution. Quasar hosts appear to be already well formed at $z \sim 2$, in disagreement with the predictions of models for the joint formation and evolution of galaxies and active nuclei based on the hierarchical structure formation scenario.

Subject headings: galaxies: active — galaxies: evolution — infrared: galaxies — quasars: general

1. INTRODUCTION

In the local universe ($z \lesssim 0.3$) images of powerful active galactic nuclei (AGNs), i.e., quasars, clearly show that they are hosted by massive galaxies. Ground-based imaging (e.g., McLeod & Rieke 1994; Taylor et al. 1996; Kotilainen & Falomo 2000; Percival et al. 2001) have been complemented by higher resolution data obtained by the *Hubble Space Telescope* (*HST*) (e.g., Disney et al. 1995; Bahcall et al. 1997; Hooper, Impey, & Foltz 1997; Boyce et al. 1998; Hutchings et al. 1999; Hamilton, Casertano, & Turnshek 2002; Dunlop et al. 2003; Pagani, Falomo, & Treves 2003) and clearly indicate that the majority of quasar hosts are massive galaxies dominated by the spheroidal component. This result is consistent with the recent discovery that nearby massive spheroids (ellipticals and bulges of early-type spirals) have an inactive supermassive black hole (BH) in their centers (see, e.g., Ferrarese 2002 for a recent review). These observations depict an evolutionary scenario where nuclear activity may be a common phenomenon during the lifetime of a galaxy with recurrent accretion episodes and the emitted nuclear power depends on the mass of the system. Powerful nuclear (quasar-like) activity is in fact found only in the most luminous (massive) galaxies (Hamilton et al. 2002; Falomo, Carangelo, & Treves 2003; Kauffmann et al. 2003).

While radio-loud quasars (RLQs) are exclusively hosted by ellipticals exceeding the characteristic galaxy luminosity L^* (Mobasher et al. 1993) by ~ 2–3 mag and similar to the brightest cluster galaxies, radio-quiet quasars (RQQ) are found both in ellipticals and in early-type spirals (Taylor et al. 1996; Bahcall et al. 1997). However, there is evidence (Dunlop et al. 2003) that at high nuclear luminosities also RQQs are hosted mainly in elliptical galaxies. There is also some indication at low redshift that the hosts of RLQs are systematically more luminous than those of RQQs (Veron-Cetty & Woltjer 1990; Bahcall et al. 1997; Dunlop et al. 2003).

The strong cosmological evolution of the quasar population (Dunlop & Peacock 1990; Warren, Hewett, & Osmer 1994; Boyle 2001) is similar to the evolution of the star formation history in the universe (Madau, Pozzetti, & Dickinson 1998; Franceschini et al. 1999; Steidel et al. 1999) and to the

number density of radio galaxies (RGs; Boyle & Terlevich 1998). This may represent the overall effect of a fundamental link between the formation of massive galaxies and the formation and fueling of their nuclei, consistent with the finding of supermassive BHs in the nuclei of nearby inactive galaxies (e.g., Kormendy & Gebhardt 2001 and references therein).

Deep high spatial resolution *HST* images of distant galaxies (e.g., Abraham et al. 1996; Koo et al. 1996; Le Fevre et al. 2000) have begun to provide data able to trace the galaxy formation, while very little is still known about the evolution of distant quasar hosts. In the present epoch, quasar activity is a rare event in galaxies, while it was a more common phenomenon at an earlier epoch ($z \sim 2-3$) when the age of the universe was only a few gigayears. This dramatic evolution of quasars must thus be connected with the formation and evolution of massive spheroids (Franceschini et al. 1999). Understanding how the properties of the galaxies hosting quasars change with the cosmic time is therefore a fundamental step to investigate the link between evolution of the galaxies and nuclear activity. In particular, it is of great importance to probe the host properties close to (and possibly beyond) the peak of quasar activity.

The detection of the host galaxies and the characterization of their properties are more and more difficult as one moves to higher redshift. This is because the surrounding nebulosity becomes rapidly very faint compared with nuclear source. This problem is critical when studying high-luminosity AGNs. In order to cope with these severe limitations, it is imperative to obtain images of the targets with the highest possible spatial resolution and sensitivity. Moreover, a well-defined point-spread function (PSF) is crucial when modeling the image of the object. These requirements are seldom matched by using ground-based medium size (4 m class) telescopes even under good seeing conditions. They are partially satisfied by *HST*, which certainly has a superbly narrow PSF but, because of its small aperture, has a relatively small throughput.

In spite of these severe difficulties, a number of studies have already been presented for quasar hosts at $z > 1$, and in some cases extended emission has been reported for quasars even at $z \gtrsim 2$ (e.g., Heckman et al. 1991; Lehnert et al. 1992, 1999; Lowenthal et al. 1995; Aretxaga, Terlevich, & Boyle 1998; Hutchings 1998, 1999). However, the results of most of these studies are limited by modest seeing and/or image deepness. A further complication may arise from the contamination, inside the broadband observed, of line emission that could originate in spatially extended regions of gas around the nucleus of the quasar. Moreover, the usually small number of objects investigated and the nonhomogeneous data sets have failed to provide an unambiguous view of the evolution of quasar hosts and of the differences between RLQ and RQQ hosts.

The most systematic study until now of high-redshift quasar host galaxies, based on *HST* NICMOS observations, has recently been presented by Kukula et al. (2001). They derived the host-galaxy luminosities for a small sample of both RLQs and RQQs at $z \sim 1$ and $z \sim 2$ and compared them with the properties of quasar hosts at lower redshift. They found that the evolution of RLQ hosts is roughly consistent with that of massive ellipticals undergoing passive evolution, while the luminosity of RQQ hosts remains nearly constant. In neither case is there a significant drop in the host mass as would be expected in the models of hierarchical formation of massive ellipticals (Kauffmann & Haehnelt 2000). Kukula et al. (2001) also find evidence for a systematic gap between RLQ and RQQ host luminosity that appears to increase with the redshift.

Taking advantage of both the excellent PSF and the high throughput of the 8 m Very Large Telescope (VLT), we have carried out a program to image and to characterize the host galaxies of quasars in the redshift range $1 < z < 2$. The first results of this program for three RLQs at $z \sim 1.5$ were reported in Falomo, Kotilainen, & Treves (2001, hereafter FKT01). In this paper we present the complete results of this program for all the 17 observed RLQs and RQQs. In § 2 we describe our observed sample, while in § 3 we report the observations and describe the data analysis. In § 4 we give our results for the observed quasars and compare them with the host luminosities of quasars derived from other samples. Finally, the cosmic evolution of RLQ and RQQ host galaxies and the relationship between host and nuclear luminosities are discussed in § 5. For consistency with previous studies, we adopt Hubble constant $H_0 = 50$ km s^{-1} Mpc^{-1} and $\Omega = 0$ throughout this paper.

2. THE SAMPLE

The observed targets were extracted from the list of objects reported in the catalog of Veron-Cetty & Veron (2001) requiring $1.0 < z < 2.0$, $-25.5 < M_B < -28$, and $-60^\circ < \delta < -8^\circ$ and having sufficiently bright stars within the observed field of view ($\sim 2'$) to allow a reliable characterization of the PSF. We included both RLQs and RQQs in order to investigate the difference between the host galaxies of the two types of quasar. We considered a sample of 26 quasars that are evenly distributed in redshift and optical luminosity. An equal number of RLQs and RQQs were taken, matching their redshift and optical luminosity distributions. In total, 14 of these sources were imaged during the two campaigns reported here (see Table 1), in addition to the three objects described in FKT01. Figure 1 shows the distribution of the observed quasars in the redshift–optical luminosity plane compared with all the quasars in the Veron-Cetty & Veron (2001) catalog. The average redshift of the observed quasars is $\langle z \rangle = 1.51 \pm 0.16$ for 10 RLQs and $\langle z \rangle = 1.52 \pm 0.16$ for seven RQQs. The average luminosity of the observed quasars is $\langle M_B \rangle = -26.75 \pm 0.73$ (rms) and $\langle M_B \rangle = -26.70 \pm 0.84$ (rms) for the RLQs and RQQs, respectively. Our observed samples are thus well matched and lie toward the high-luminosity end of the quasar in the Veron-Cetty & Veron (2001) catalog.

To perform the comparison between the hosts of RLQs and RQQs, it is important to ensure that the RLQs are genuinely radio-loud [$P(5\ \mathrm{GHz}) > 10^{25}$ W Hz^{-1} sr^{-1}] and that the RQQs are genuinely radio-quiet [$P(5\ \mathrm{GHz}) < 10^{24.5}$ W Hz^{-1} sr^{-1}]. For our sample of RLQs the average 5 GHz (6 cm) radio luminosity is $\langle \log P(5\ \mathrm{GHz}) \rangle$ (W Hz^{-1} sr^{-1}) $= 27.18 \pm 0.40$ (rms). Note that even the radio-faintest of the RLQs [$\log P(5\ \mathrm{GHz}) = 26.3$ W Hz^{-1} sr^{-1}] is well beyond the threshold for radio loud objects. No radio data are available for the RQQs in the sample both from the QSO catalog and from NED.

Of the 10 RLQs, eight are steep-spectrum radio quasars (SSRQs; $\alpha < 0$) and two are flat-spectrum radio quasars (FSRQs; $\alpha > 0$). The average 6–11 cm radio spectral index of the observed RLQs is $\langle \alpha(6-11\ \mathrm{cm}) \rangle = -0.18 \pm 0.64$ (rms).

TABLE 1
JOURNAL OF OBSERVATIONS

Quasar	z	V[a]	Date	Filter	T_{exp}[b] (min)	Seeing[c] (arcsec)
Radio-quiet Quasars						
Q0040−3731.....	1.780	17.8	2001 Jun 9	*K*	38	0.37
			2001 Aug 16	*K*	36	0.56
HE 0935−1001.....	1.574	17.6	2002 Jan 15	*K*	36	0.46
			2002 Jan 15	*K*	36	0.46
			2002 Jan 15	*K*	36	0.47
			2002 Jan 15	*K*	36	0.48
0119−370.....	1.320	19.2	2001 Aug 10	*H*	30	0.44
			2001 Aug 16	*H*	30	0.53
0152−4055	1.650	19.3	2001 Aug 9	*K*	36	0.33
			2001 Aug 19	*K*	36	0.37
LBQS 2135−42.....	1.469	18.35	2001 May 30	*K*	36	0.38
			2001 Jul 4	*K*	36	0.33
Q2251−2521.....	1.341	17.7	2001 Jul 5	*H*	36	0.51
Q2348−4012.....	1.500	19.5	2001 Jul 8	*K*	36	0.48
			2001 Jul 8	*K*	36	0.44
Radio-loud Quasars						
PKS 0100−27.....	1.597	17.8	2001 Aug 16	*K*	36	0.58
			2001 Aug 18	*K*	30	0.39
PKS 0155−495.....	1.298	18.4	2001 Aug 19	*H*	36	0.39
PKS 1018−42.....	1.280	18.9	2002 Jan 21	*H*	38	0.33
PKS 1102−242.....	1.660	19.3	2002 Jan 19	*K*	28	0.38
			2002 Jan 26	*K*	28	0.38
PKS 1511−10.....	1.513	18.5	2002 May 16	*K*	36	0.32
			2002 May 16	*K*	36	0.36
PKS 2210−25.....	1.833	19.0	2001 Jun 23	*K*	36	0.37
			2001 Jul 4	*K*	36	0.37
PKS 2227−08.....	1.562	17.5	2001 Jul 12	*K*	34	0.34
			2001 Jul 5	*K*	30	0.42

[a] Quasar *V*-band magnitudes from the Veron-Cetty & Veron 2001 catalog.
[b] Frame exposure time in minutes
[c] The average FWHM in arcsec, of all stars in the frame.

Given the small fraction of FSRQs, we assume that beaming effects for the nuclear emission are negligible.

3. OBSERVATIONS

Deep images of the quasars in the *H* or *K* bands were obtained using the near-infrared (NIR) ISAAC camera (Cuby et al. 2000), mounted on the first 8 m unit telescope (UT1, Antu) of VLT at the European Southern Observatory (ESO) in Paranal, Chile. At the redshift of the objects, the observed bands correspond to rest-frame *R* and *I* bands, where most of the studies for low-redshift objects have been performed. The short-wavelength arm of ISAAC is equipped with a 1024×1024 pixel Hawaii Rockwell array, with a pixel scale of $0\farcs147$ pixel^{-1}, giving a field of view of $\sim 150'' \times 150''$. The observations were performed in service mode in the period 2001 June to 2002 May.

A detailed journal of the observations is given in Table 1. The seeing, as derived from the median FWHM size of the image of stars in each frame, was consistently excellent during all observations, ranging from $\sim 0\farcs32$ to $\sim 0\farcs58$ (average $\langle \mathrm{FWHM} \rangle = 0\farcs41$; median $= 0\farcs39$).

Total integration times were $\sim$60 and $\sim$30 minutes for targets above and below $z = 1.4$, respectively. To maintain the stability of the observing conditions (in particular of the seeing) during the integration time, we typically obtained pairs of images of $\sim$30 minutes each to reach the 60 minutes of total integration. The images were secured using a jitter procedure and individual exposures of 2 minutes per frame. The jittered observations were controlled by an automatic template (see Cuby et al. 2000), which produced a set of frames slightly offset in telescope position from the starting point. The observed positions were randomly generated within a box of $10'' \times 10''$ centered on the first pointing. Each frame was flat-fielded and sky-subtracted, and the final image was produced for each quasar by co-adding these frames. Data reduction was performed by the ESO pipeline for jitter imaging data (Devillard 1999). The normalized flat field was obtained by subtracting ON and OFF images of the illuminated dome, after interpolating over bad pixels. Sky subtraction was done by median-averaging sky frames from the 10 frames nearest in time. The reduced frames were aligned to subpixel accuracy using a fast-object detection algorithm and co-added after removing spurious pixel values. Photometric calibration was performed using standard stars observed during the same night. The estimated internal photometric accuracy is ± 0.03 mag. We have also performed an additional check of the photometric calibration based on field stars that have NIR magnitudes in the Two Micron All Sky Survey (2MASS) point-source catalog. We find three or four stars in the fields of PKS 2210−25, PKS 2227−08,

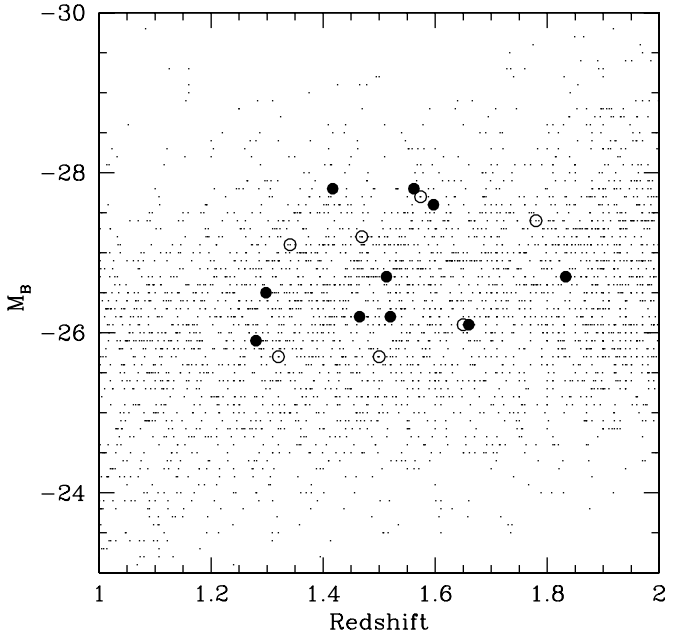

FIG. 1.—Distribution of the observed quasars in the z-M_B plane, compared with quasars in the Veron-Cetty & Veron (2001) catalog. The RLQs (*filled circles*) and RQQs (*open circles*) in our sample share an identical distribution in terms of redshift and optical luminosity.

and PKS 1511−10. The agreement between 2MASS and our photometry is in all cases within 0.1 mag. For three objects in the sample we found previous NIR photometry published in the literature (Francis, Whiting, & Webster 2000): the photometry obtained through a 5″ aperture ($K = 14.70$ for PKS 1511−100, $K = 15.65$ for PKS 2210−257, and $K = 15.06$ for PKS 2227−088) differs by 0.1–0.7 mag with ours (see Table 2), indicating a moderate NIR nuclear variability.

The use of the H and K bands combined with observing in the $1.3 < z < 1.8$ redshift interval implies that we are sampling a rest-frame interval of ∼300 Å between 6500 and 8900 Å, depending on the redshift of the object. In this region the only relevant strong emission line is Hα at 6563 Å. The averaged rest-frame wavelength sampled for the seven RLQs and seven RQQs presented here varies between 7000 and 8900 Å and excludes this emission line. Note, however, that for the three $z \sim 1.5$ RLQs studied by FKT01 in the H band, some contamination from the Hα line may be present.

4. DATA ANALYSIS

To detect and characterize the properties of the host galaxies of quasars, the key factors are the apparent nucleus-to-host magnitude ratio and the seeing (shape of the PSF). While the total magnitudes of the hosts are relatively easily determined, the scale lengths are less well constrained. The most critical part of the analysis is to perform a detailed study of the PSF for each frame. In particular, it is important to have a sufficient number of reference stars distributed over the field of view in order to account for any possible positional dependence of the PSF. Moreover, it is essential to have at least one sufficiently bright star in the field to allow a reliable evaluation of the shape of the faint wing of the PSF, against which most of the signal from the surrounding nebulosity will be detected.

The relatively large field of view of ISAAC (∼2.′5) and the constraint on the quasar selection to have at least one bright star in the field of view allowed us to reach this goal and thus to perform a trustworthy characterization of the PSF. For each field, we analyzed the shape of all stellar

TABLE 2
RESULTS OF THE RADIAL PROFILE MODELING

Quasar	z	Filter	$m_{\rm nuc}$[a]	$m_{\rm host} \pm \Delta m_{\rm host}$[a]	$r_e \pm \Delta r_e$[b] (arcsec)	χ^2_ν(PSF)/χ^2_ν(Fit)[c]
Radio-quiet Quasars						
Q0040−3731	1.780	K	15.5	19.4 0.3	(1.3)	6.2
HE 0935−1001	1.574	K	15.1	>19.5		1.0
0119−370	1.320	H	18.1	19.1 ± 0.2	1.0 ± 0.4	27.5
0152−4055	1.650	K	17.1	18.6 ± 0.3	1.6 ± 1.0	16.0
LBQS 2135−42	1.469	K	15.9	18.7 ± 0.4	1.3 ± 1.0	5.1
Q2251−2521	1.341	H	16.0	18.5 ± 0.4	1.6 ± 0.7	9.3
Q2348−4012	1.500	K	16.9	19.5 ± 0.6	(1.1)	9.7
Radio-loud Quasars						
PKS 0100−27	1.597	K	15.7	18.5 ± 0.5	0.5 ± 0.2	6.5
PKS 0155−495	1.298	H	17.8	18.4 ± 0.2	0.5 ± 0.3	30.7
PKS 1018−42	1.280	H	15.9	17.6 ± 0.3	1.4 ± 0.6	25.2
PKS 1102−242	1.660	K	14.9	18.1 ± 0.6	(1.7)	5.8
PKS 1511−10	1.513	K	14.8	18.2 ± 0.4	(1.8)	5.0
PKS 2210−25	1.833	K	16.1	19.3 ± 0.3	1.2 ± 1.0	2.9
PKS 2227−08	1.562	K	15.8	18.9 ± 0.3	0.3 ± 0.2	3.8

[a] Apparent magnitudes correspond to the indicated filter.
[b] Effective radii are reported in parentheses when the value is uncertain because of the degeneracy of the best-fit parameters.
[c] The ratio between the reduced χ^2_ν value of the fit with only the PSF model and that of the fit with PSF and host-galaxy model. Only in the case of HE 0935−1001 does the χ^2 not significantly improve when adding the galaxy component; therefore HE 0935−1001 is indicated as unresolved.

profiles and constructed a composite PSF, the brightness profile of which extends down to $\mu_K \sim 24.5$ mag arcsec^{-2}. This guarantees a reliable comparison between the luminosity profiles of the quasars and of the stars without requiring blind extrapolation of the PSF at large radii (faint fluxes) that could produce spurious results. The shape of the PSF profile was found to be symmetric (ellipticity less than few percent) and very stable across the field of the images. The differences of FWHM of the stars in each frame were typically less than a few percent, while no significant difference was found among their radial brightness profiles. In Figure 2 we show an example of the azimuthally averaged radial profiles of stars used to construct a PSF, together with the overall deviations from the used PSF model of individual stellar profiles.

In all our objects the emission from nuclear source is clearly dominant with respect to the light from the extended surrounding nebulosity. A first indication of the presence of a surrounding nebulosity can be obtained after the subtraction of a scaled PSF. However, visual inspection of these PSF-subtracted images allow one to see residual emission only for the objects where the contrast between nucleus and host galaxy is relatively low (see the examples reported in Fig. 3).

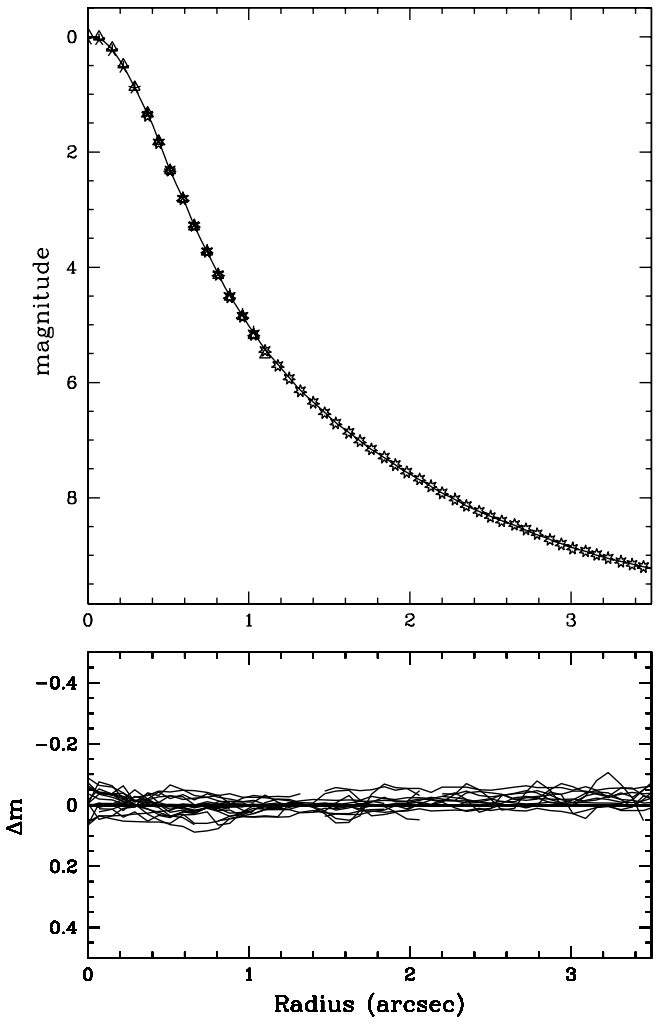

FIG. 2.—*Top:* The PSF radial brightness profile (*solid line*) for the field of Q2348−4012, compared with the radial profiles of individual stars (*triangles, stars, and crosses*) in the frame. *Bottom:* Differences between the stellar radial brightness profiles and the adopted PSF model for all frames.

In other cases the high contrast of the components (nucleus and host) of the objects prevents clear visualization of the extended nebulosity above the signal-to-noise ratio (S/N) per pixel of the images.

In order to improve the S/N of the data and the capability to detect the faint signal from the host galaxies we have therefore computed for each quasar the azimuthally averaged fluxes as a function of the distance from the nucleus, excluding any region around the quasars contaminated by companion objects. These companions are easily recognized from the original and PSF-subtracted images since they are in all cases rather compact features covering an area of few tenths of arcsecond in the image. To perform this cleaning we substituted the area contaminated by possible companions with the corresponding one in the image that is symmetric with respect to the center of the target. In this way we avoid also removing the emission from the underlying galaxy and assume that it is essentially regular. With this procedure we obtained the radial luminosity profile out to a radius where the signal becomes indistinguishable from the background noise. For our observations, this level corresponds to $\mu(K) \sim 23$–24 mag arcsec^{-2}, typically reached at $\sim 2''$–$3''$ distance from the nucleus. This procedure allowed us to significantly improve the S/N at the faint fluxes where the signal from the host galaxy becomes detectable with respect to that from the unresolved nuclear source.

A straightforward comparison of the average radial brightness profile with that of the proper PSF gives us a first indication of the amount of the extended emission. Detailed modeling of the luminosity profile was then carried out using an iterative least-squares fit to the observed profile, assuming a combination of a point source (modeled by the PSF) and an elliptical galaxy described by a de Vaucouleurs $r^{1/4}$ law, convolved with the proper PSF.

We also attempted a fit using a pure exponential disk model for the host galaxy. Note, however, that the small extent of the hosts and the dominance of the nuclear emission of the observed targets make it very difficult to discriminate between the two models. Nevertheless, in all cases where the object is well resolved, we find that the elliptical model yields a better fit than a disk model. Therefore, based on this, and consistently with the properties of lower redshift RLQs, we have assumed the elliptical model for the determination of the host-galaxy properties in the following discussion. If a disk model were assumed, the luminosities of the hosts would systematically become ~ 0.3 mag fainter. This difference does not affect the main conclusions of this study.

With the applied procedure we can derive the luminosity and the scale length of the host galaxies and the luminosity of the nuclei. We have estimated the accuracy of the decomposition to derive the host parameters, taking into account the uncertainty of the observed profile (which is limited mainly by the S/N at the faintest flux levels) and the accuracy of the PSF shape. We assumed the uncertainty in the derived parameters for a variation of $\chi^2_\nu = 2.7$ (for 2 degrees of freedom). While the total magnitude of the host galaxy can be derived with a typical internal error of 0.2–0.3 mag, the scale length is often poorly constrained. This depends on the degeneracy that occurs between two model parameters: the effective radius r_e and the surface brightness μ_e. In fact, for a given value of the total magnitude of the host, various pairs of r_e and μ_e can fit the data without a significant difference in the χ^2_ν value (see also Abraham, Crawford, & McHardy 1992; Taylor et al.

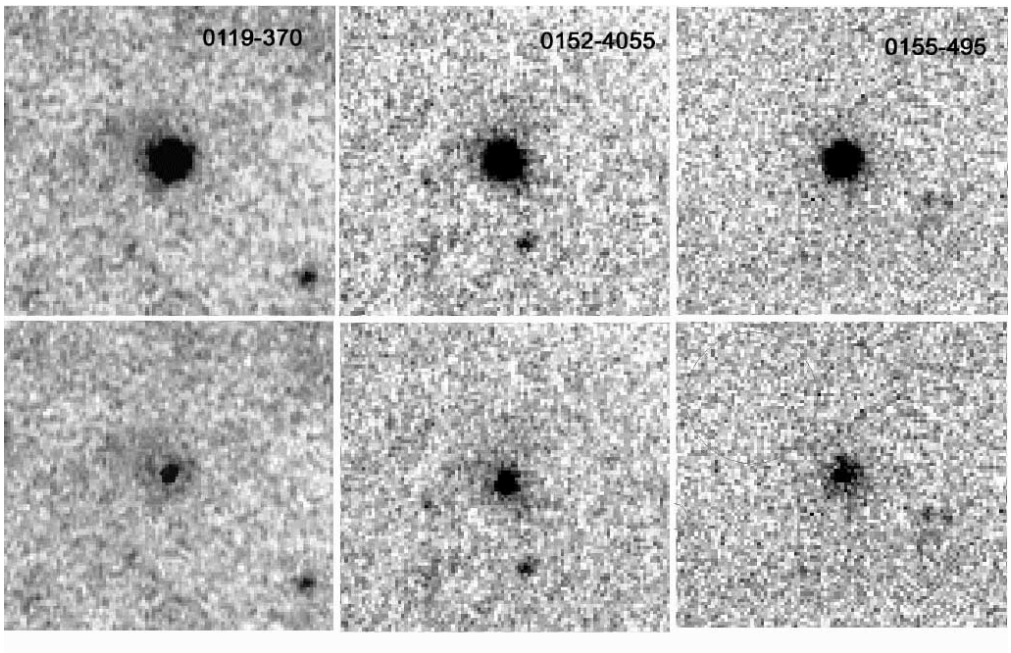

FIG. 3.—*Top:* Near-IR images of three QSOs in the sample. The full size of the images in each panel is 15″. North is up, and east to the left. The central panel shows an example of two close companion objects around a quasar that have been removed in the analysis of the host galaxy (see text). *Bottom:* Same as above, but after subtraction of a scaled PSF.

1996; Dunlop et al. 2003; Pagani et al. 2003 for further discussion on this issue).

5. RESULTS

In Figure 4 we report for each quasar the observed radial brightness profile and the best fit using the elliptical galaxy model and the procedure described above. The parameters of the best fit, together with their estimated uncertainty, are given in Table 2. For all quasars except one (HE 0935−1001) we find significant systematic deviations of the radial profile with respect to its proper PSF. This is quantified in Table 2 by the ratio of the reduced χ^2_ν value of the best fit with that obtained from the fit excluding the galaxy component, i.e., considering only the PSF.

In Table 3 we give the absolute magnitudes and the effective radii for each quasar host, including the three RLQs analyzed in FKT01. The absolute magnitudes of the host galaxies have been *K*-corrected using the optical-NIR evolutionary synthesis model for elliptical galaxies (Poggianti 1997). For the nuclear magnitudes we applied a correction $\Delta m = -2.5(\alpha + 1)\log(1 + z)$. No correction for Galactic extinction was applied since it is negligible in the observed NIR bands. Moreover, to make the results homogeneous we transformed the *H*-band magnitudes to the *K* band, assuming an intrinsic color $H-K = 0.2$ typical of ellipticals and $H-K = 1$ for the nucleus.

5.1. *Host Galaxies of RLQs and RQQs between $z = 1$ and $z = 2$*

In the following we describe the properties of our full sample of 16 resolved quasars. The average absolute *K*-band magnitude of the host galaxies is $\langle M_K\rangle(\text{host}) = -27.55 \pm 0.12$ and $\langle M_K\rangle(\text{host}) = -26.83 \pm 0.25$ for the RLQs and RQQs, respectively. The average absolute *K*-band magnitude of the nuclei after taking into account the above-mentioned *K*- and color corrections is $\langle M_K\rangle(\text{nucleus}) = -30.94 \pm 1.2$ and $\langle M_K\rangle(\text{nucleus}) = -30.20 \pm 1.2$ for the RLQs and RQQs, respectively.

We plot in Figure 5 the absolute *K*-band magnitude of the quasar host galaxies versus the redshift. All the observed quasars have host galaxies with luminosity ranging between M^* and $M^* - 2$, where $M^*(K) = -25.2$ (Mobasher, Sharples, & Ellis 1993) is the characteristic luminosity of the Schechter luminosity function for elliptical galaxies. For comparison, we also report in Figure 5 the absolute magnitudes of four RLQs and five RQQs at $z \sim 1.9$ (Kukula et al. 2001) and three RQQs at $z \sim 1.8$ (Ridgway et al. 2001), derived from *HST* NICMOS imaging studies. Note that the objects in these samples cover a large range in nuclear luminosity and are on average less luminous than those in the sample considered here. In order to treat these literature data homogeneously, we have considered the published apparent magnitudes in the *J* and *H* bands (*HST* filters F110M and F165M) and transformed them to M_K following our procedure (*K*-correction, cosmology, and color correction). In particular, we converted the *H*-band magnitudes in Table 2 of Kukula et al. (2001), which are in the *HST* magnitude system (K. Kukula 2003, private communication) into the standard IR Johnson system. To do this, we computed synthetic color transformations from the F110M and F160M *HST* filters to the *J* and *H* bands assuming the input spectrum of an elliptical galaxy (Kinney et al. 1996) and the passband curves of the filters. This yields a correction of ∼0.5 and ∼0.2 mag for the *J* and *H* bands, respectively. For the three RQQs observed by Ridgway et al. (2001), we converted their published *H*-band fluxes into *H*-band magnitudes and then applied the corrections to the aperture magnitudes (their Tables 3 and 5) to obtain the total magnitudes of the hosts. Note that all the *HST* data show a substantially larger scatter than our VLT data. In particular, four of the five RQQs observed by Kukula et al. (2001) lie above M^*, while all

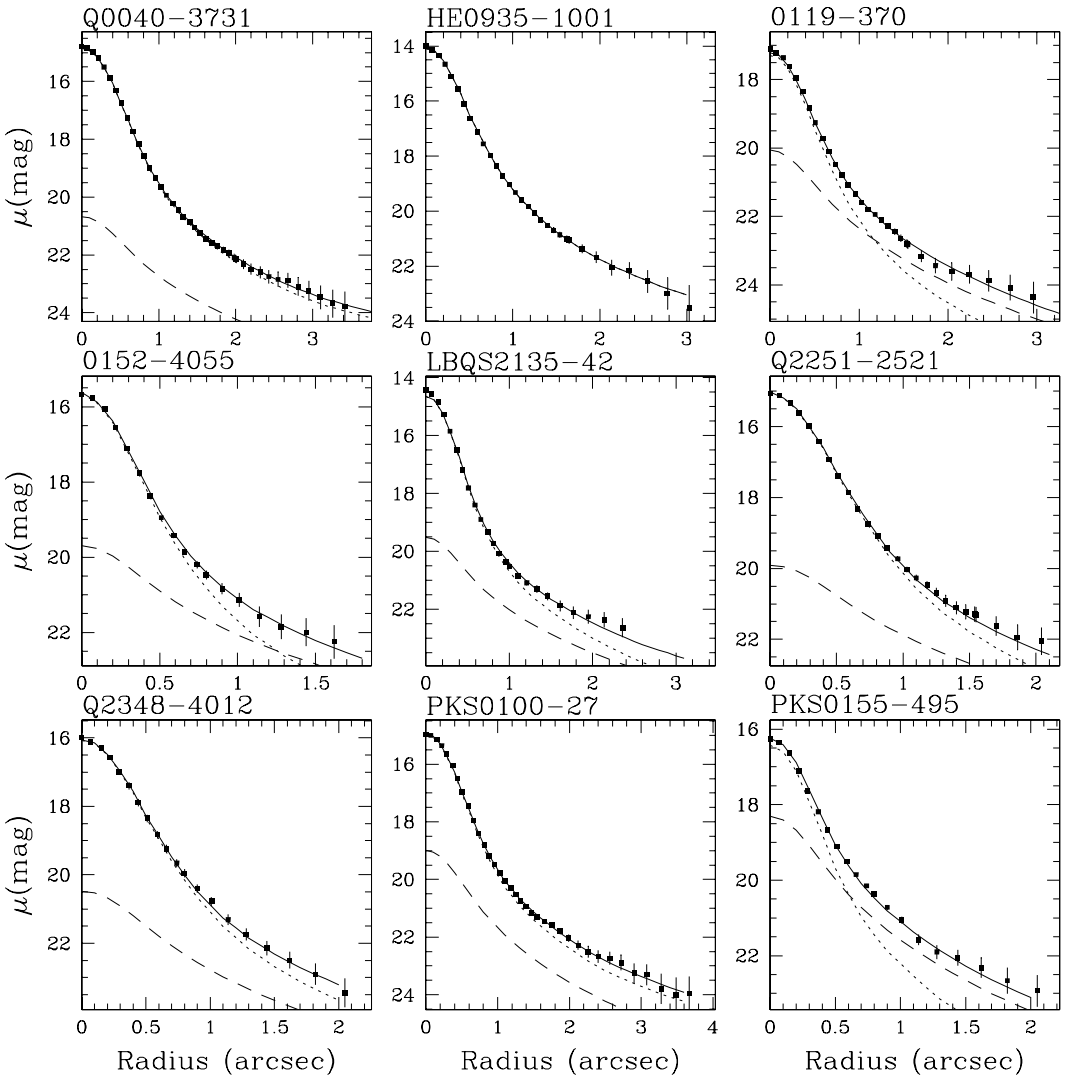

FIG. 4.—Observed radial brightness profiles of the quasars (*filled squares*), superposed on the fitted model consisting of the PSF (*dotted line*) and an elliptical (de Vaucouleurs law) galaxy convolved with its PSF (*dashed line*). The solid line shows the composite model fit.

three RQQs observed by Ridgway et al. (2001) are at or below M^*. The reason for this larger scatter is unclear but could be partially related to nonhomogeneous data analysis. While the host parameters in this work and in Kukula et al. (2001) are derived using (one- or two-dimensional) modeling of the brightness distribution of the sources, the measurements of Ridgway et al. (2001) are obtained from aperture fluxes and, in spite of the applied corrections, could still underestimate the host-galaxy luminosity. On the other hand the nuclei of two of the three objects studied by Ridgway et al. (2001) are about 4 mag fainter than the average luminosity of the objects in our sample. This may suggest some dependence of the host-galaxy luminosity on the nuclear luminosity. The available data are, however, too scanty to properly assess this point (see also § 5.3 for further discussion).

Based on our VLT results, we find a systematic difference in the luminosity between RLQ and RQQ host galaxies of a factor $\sim$2 ($\sim$0.7 mag). Similar difference was already noted by previous studies for quasars at lower redshift (Veron-Cetty & Woltjer 1990; Bahcall et al. 1997; Dunlop et al. 2003) and comparably high redshift (Kukula et al. 2001). Whether this difference is intrinsic or due to some selection effect has been long discussed (e.g., Hutchings, Crampton, & Campbell 1984; Smith et al. 1986; Veron-Cetty & Woltjer 1990; Taylor et al. 1996; Hooper et al. 1997; Kirhakos et al. 1999; Dunlop et al. 2003; Sanchez & Gonzalez-Serrano). Main biases invoked to explain the difference are the nonhomogeneous distribution in redshift, optical luminosity, or modeling of the host galaxy (elliptical vs. disk systems) of the compared samples. Our RLQ and RQQ subsamples span the same range in redshift and optical luminosity, and therefore these effects are irrelevant. Our results, together with those of Bahcall et al. (1997), Kukula et al. (2001), and Dunlop et al. (2003), therefore strongly indicate that the difference in host luminosity is intrinsic and remains the same over a wide range of redshift.

For the effective radius of the host galaxies, we formally find $\langle R_e \rangle = 10.4 \pm 7.7$ kpc (RLQ) and $\langle R_e \rangle = 16.3 \pm 3.4$ kpc (RQQ), the reported uncertainties being the dispersion of the distribution, while the individual large errors have not been taken into account. The host galaxies of our high-redshift quasars appear to be on average quite large, much larger than those found in earlier studies (FKT01; Ridgway et al. 2001) and similar to those of intermediate-redshift RLQs (Kotilainen, Falomo, & Scarpa 1998; Kotilainen & Falomo

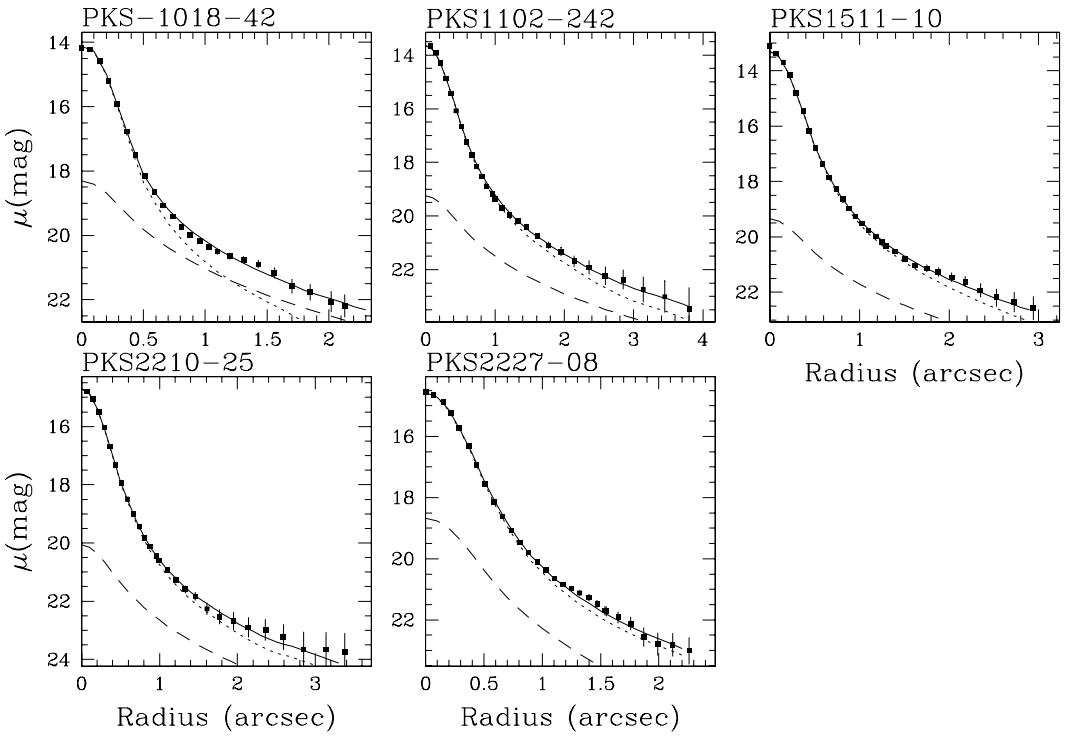

FIG. 4.—*Continued*

TABLE 3

PROPERTIES OF THE QUASARS AND THEIR HOST GALAXIES

Quasar	z	μ_e[a,b]	K-correction[c]	$M_{\rm nucl}$[d]	$M_{\rm host}$[c]	R_e[d] (kpc)
Radio-quiet Quasars						
Q0040−3731	1.780	(23.7)	−0.27	−31.5	−26.8	(16)
0119−370	1.320	22.3	0.06	−28.9	−26.7	11.8
0152−4055	1.650	23.4	−0.30	−29.6	−27.3	20.7
LBQS 2135−42	1.469	(22.6)	−0.32	−30.4	−26.9	(16)
Q2251−2521	1.341	22.7	0.07	−31.1	−27.4	19.6
Q2348−4012	1.500	(23.7)	−0.32	−29.5	−26.1	(13)
Radio−loud Quasars						
PKS 0000−177[e]	1.465	19.1	0.12	−30.4	−27.5	3.6
PKS 0100−27	1.597	20.9	−0.31	−31.0	−27.3	6.8
PKS 0155−495	1.298	19.9	0.05	−29.1	−27.4	5.7
PKS 0348−120[e]	1.520	19.7	0.15	−30.4	−27.8	4.9
PKS 0402−362[e]	1.417	19.0	0.10	−32.1	−27.9	4.1
PKS 1018−42	1.280	21.5	0.04	−31.0	−28.1	16.5
PKS 1102−242	1.660	(22.9)	−0.30	−31.9	−27.9	(21)
PKS 1511−10	1.513	(23.3)	−0.32	−31.7	−27.5	(22)
PKS 2210−25	1.833	(23.3)	−0.26	−31.0	−27.0	(15)
PKS 2227−08	1.562	20.0	−0.31	−30.7	−26.9	3.7

[a] Surface brightness at the effective radius (mag arcsec^{-2}) derived from the best-fit model.
[b] Values enclosed in parentheses are uncertain (see text).
[c] K-correction of the host galaxy from Poggianti 1997.
[d] Absolute magnitudes of the host galaxies and the nuclei are given in the K band assuming $H_0 = 50$ km s^{-1} Mpc^{-1} and $\Omega = 0$. The magnitudes are $K-$corrected as described in the text and no correction for galactic extinction is applied.
[e] Results from FKT01.

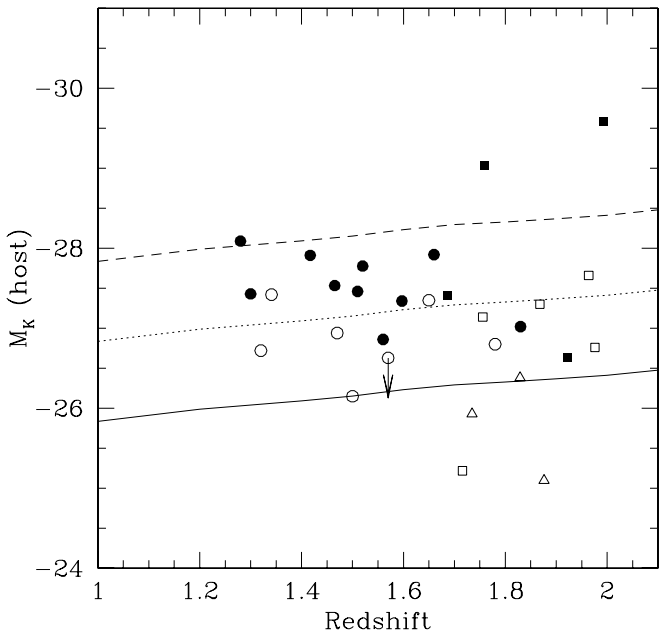

FIG. 5.—*K*-band absolute magnitude of the host galaxies of observed quasars vs. redshift. Hosts of RLQs (*filled circles*) and RQQs (*open circles*) from this work are confined to the range between M^* and $M^* - 2$. The arrow represents the upper limit of the host luminosity for the unresolved object HE 0935−1001. The lines represent the expected behavior of a massive elliptical (at M^*, $M^* - 1$, and $M^* - 2$; *solid, dotted, and dashed lines*) undergoing simple passive evolution (Bressan et al. 1998). Also included are the four RLQs (*filled squares*) and five RQQs (*open squares*) at $z \sim 1.9$ from the *HST* study of Kukula et al. (2001) and three RQQs (*open triangles*) from Ridgway et al. (2001).

2000). However, given that R_e is poorly constrained because of the degeneracy between R_e and μ_e, we stress that the apparent difference in R_e between RLQs and RQQs has to be considered with caution.

5.2. *The Evolution of Quasar Hosts*

In order to investigate the evolution of the host luminosity of RLQs and RQQs up to $z = 2$, we report in Figure 6*a* the average luminosities of host galaxies derived from various quasar samples at $z < 2$. We prefer to consider (when available) the results from *HST* NIR studies, which are in general more homogeneous than those based on ground-based data. When a sizeable sample is not available from *HST* imaging, we used NIR ground-based data. A further criterion in selecting data to use is that total apparent magnitudes of the host galaxies must be available. This is required in order to perform a homogeneous treatment of the data.

In the range from $z = 1$ to $z = 2$, in addition to the average values from this study, we use the data from the studies by Kukula et al. (2001) and Ridgway et al. (2001) described above. At lower redshift, we have considered data from the study of all RLQ hosts (34 objects) at $z < 0.5$ imaged with *HST* (Pagani et al. 2003) that include previous *HST* studies of RLQ hosts by Bahcall et al. (1997), Boyce et al. (1998), and Dunlop et al. (2003) and from the study of 12 RQQs at $z \sim 0.15$ by Dunlop et al. (2003). We also report the results on six RLQs and 10 RQQs at $z \sim 0.5$ studied by Hooper et al. (1997) using *HST* WFPC2 and the F675W (*R*) filter. Moreover, we also added the average value of two extensive studies of RLQ hosts in the NIR at $0.5 < z < 1.0$ (Kotilainen, Falomo, & Scarpa 1998; Kotilainen & Falomo 2000). All these data have been made consistent with our system (as regards extinction, *K*-correction, and cosmology) starting from the total apparent magnitudes of the host galaxies.

We show in Figure 6 how the average host luminosities for the quasar samples described above evolve with redshift. It turns out that (within the uncertainties of the data) the host galaxies of both types of quasars follow the expected passive evolution of massive ellipticals, with RLQ hosts being a factor of $\sim$2 more luminous than RQQ hosts. Between $z = 0$ and $z = 2$ there is no indication of a systematic change in the luminosity gap between RLQ and RQQ hosts (see also Fig. 5). Note that both the RLQ and RQQ data from Hooper et al. (1997) appear to lie slightly but systematically below (fainter hosts) the overall trend defined by the other quasar samples. The same trend is also apparent from comparison of their apparent magnitudes in the Hubble diagram (see Fig. 7). It is also worth noting that the increase by $\sim$0.5 mag of the luminosity gap between $z = 1$ and $z = 2$ proposed by Kukula et al. (2001) critically depends on one RQQ in their sample that is hosted by a particularly faint galaxy (see also Fig. 5). The difference between RLQ and RQQ hosts at $z \sim 2$ thus appears to be comparable with the gap at lower redshift within the relatively large uncertainty in the average values. In Figure 6*a* the data for the three RQQs studied by Ridgway et al. (2001) seem to substantially deviate from the rest of the data. Apart from the possible underestimation of the host-galaxy contribution discussed above, it is worth noting that two of the three quasars are significantly less luminous (by $\sim$3 mag) than the average of the other high-redshift quasars considered here (see also next section). Possible effects due to differences in the nuclear luminosity cannot thus be excluded.

We therefore believe that the present data indicate that the difference between RLQ and RQQ hosts does not significantly depend on redshift, at least up to $z \sim 2$. This scenario of a passive evolution of quasar hosts is consistent with the few available spectroscopic studies of low-redshift quasar hosts and RGs (e.g., Canalizo & Stockton 2000; Nolan et al. 2001; de Vries et al. 2000), indicating that their stellar content is dominated by an old well-evolved stellar population. Finally, we note that these results do not change significantly if instead of the adopted cosmology we use the currently popular cosmology with $H_0 = 72$ km s^{-1} Mpc^{-1}, $\Omega_m = 0.3$, and $\Omega_\lambda = 0.7$ (see Fig. 6*b*).

A cosmic luminosity evolution, similar to that of the quasar hosts, is also displayed by RGs at least out to $z \sim 2.5$ (Best, Longair, & Röttgering 1998; Lacy, Bunker, & Ridgway 2000; Pentericci et al. 2001; Willott et al. 2003; Zirm, Dikinson, & Dey 2003), whereas at even higher redshift ($z > 3$) there is evidence that RGs have disturbed morphologies and a large spread in luminosity (Pentericci et al. 2001; van Breugel et al. 1999; Lacy et al. 2000). In Figure 7 we show the location of the RLQ hosts studied in this work and the hosts of various other RLQ samples at low and high redshift, in the NIR apparent magnitude versus redshift diagram, relative to the established relation for RGs (Willott et al. 2003 and references therein). For comparison, we also show the evolutionary model for elliptical galaxies derived from passive stellar evolution models (Bressan, Granato, & Silva 1998). The high-redshift RLQ hosts studied here fit remarkably well to the upper end of the RG *K*-redshift relation, better than those in Kukula et al. (2001) and well within the scatter for RGs themselves. On the other hand, there is much larger scatter for RLQs at intermediate redshift, although the average value for

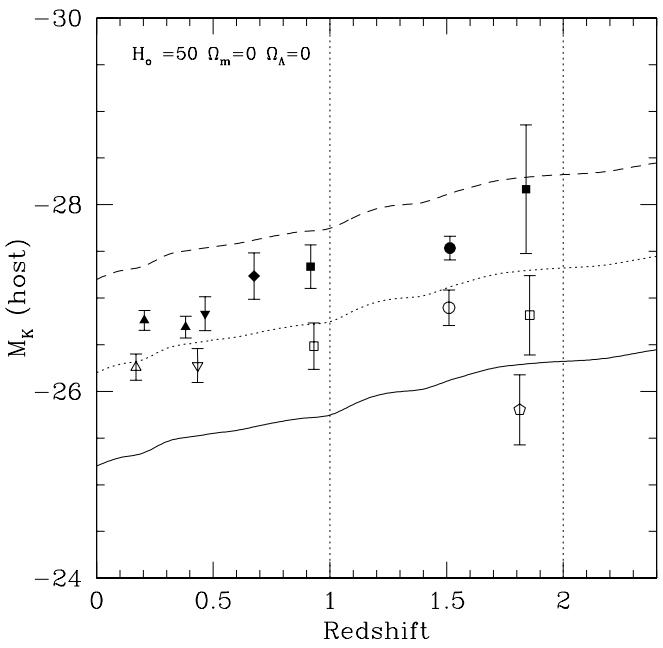

FIG. 6*a*

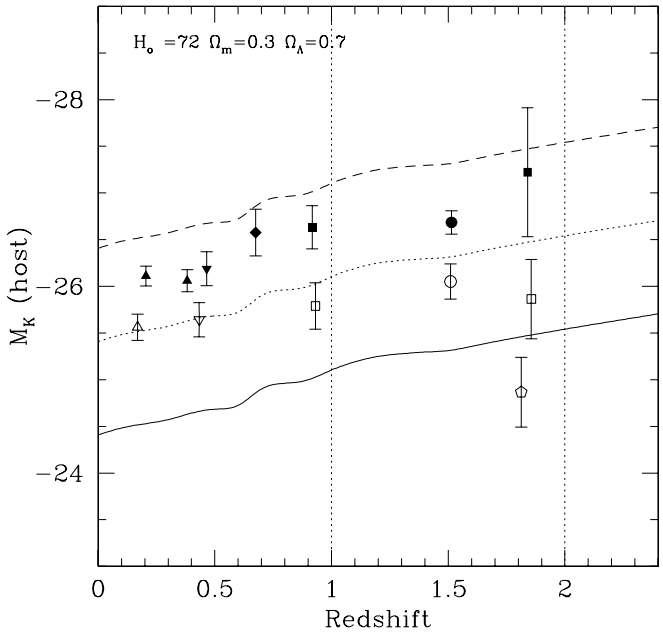

FIG. 6*b*

FIG. 6.—(*a*) The evolution of quasar host luminosity compared with that expected for massive ellipticals assuming $H_0 = 50\Omega_m = 0\Omega_\Lambda = 0$. Both RLQs (*filled symbols*) and RQQs (*open symbols*) appear to follow the standard passive evolution for luminous elliptical galaxies. Data from this work (*circles*) are compared with quasar at $z \sim 0.9$ and $z \sim 1.9$ from the *HST* study of Kukula et al. (2001; *filled squares*); FSRQ and SSRQ study at $z \sim 0.8$ from Kotilainen, Falomo, & Scarpa (1998) and FKT01 (*filled diamonds*); low-redshift RLQs compiled from *HST* observations Pagani et al. (2003; *filled triangles*) divided in two bins (objects at redshift smaller and larger than $z = 0.25$); low-redshift RQQs from Dunlop et al. (2003; *open triangles*) and three RQQs at $z \sim 1.8$ (*open pentagons*) by Ridgway et al. (2001); data for $z \sim 0.5$ are taken from Hooper et al. (1997; *inverted filled triangle for RLQs and inverted open triangles for RQQs*). Each point is plotted at the mean redshift of the considered sample, while the error bar represents the dispersion of the mean value of the host luminosity. The lines represent the expected behavior of a massive elliptical (at M^*, $M^* - 1$, and $M^* - 2$; *solid, dotted, and dashed lines*) undergoing passive stellar evolution (Bressan et al. 1998). (*b*) Same as (*a*) but using the cosmology $H = 50$, $\Omega_m = 0.3$, and $\Omega_\Lambda = 0.7$.

RLQ hosts agrees reasonably well with that of the RGs. Both RGs and RLQs therefore appear to follow the same Hubble relation, indicating that both types of AGNs are hosted by similar old massive elliptical galaxies.

The cosmic evolution traced by quasar hosts up to $z \sim 2$ disagrees with the expectations of semianalytic models of AGN and galaxy formation and evolution based on the hierarchical scenario (e.g., Kauffmann & Haehnelt 2000). These models predict fainter (less massive) hosts at high redshift, which then merge and grow to form the massive spheroids observed in the present epoch. On the other hand, our results indicate that the luminosities of both RLQ and RQQ hosts are confined within a relatively small (∼2 mag) range (see Figs. 5 and 6). This seems in agreement with the above hierarchical model that predicts a small scatter in the absolute magnitude for high-luminosity quasar hosts.

Thus, if quasar hosts are luminous spheroids undergoing passive evolution, their mass remains essentially unchanged from $z \sim 2$ up to the present epoch. This scenario is consistent with the results of recent deep surveys of distant galaxies that do not find indication of a drop of massive galaxies at high-redshift (Cimatti 2003). Alternatively, one could assume a more complex picture in which the mass of the hosts has increased from $z \sim 2$ to $z = 0$ because of merger processes, as expected in the hierarchical models, and that at the same time their stellar content is much younger and more luminous, such as to mimic the passive evolution behavior. However, the observed dominance of old stellar population in nearby quasar host galaxies and their structural properties do not favor this interpretation. Unfortunately, no data are available on the stellar content for high-redshift quasars to further assess this point.

5.3. *Nuclear versus Host Properties*

Assuming that the mass of the central BH is proportional to the luminosity of the spheroidal component of the galaxy, as is observed for nearby massive early-type galaxies (Kormendy & Richstone 1995; Magorrian et al. 1998; Kormendy & Gebhardt 2001), and that the quasar is emitting at a fixed fraction of the Eddington luminosity, one would expect a correlation between the luminosity of the nucleus and that of the host galaxy. However, the combined effects of nuclear obscuration, possible beaming, and an intrinsic spread in accretion rate and mass-to-luminosity conversion efficiency may destroy this correlation.

Our sample was designed to explore a broad range of nuclear luminosities ($-25.5 < M_B < -28$) and can therefore be used to investigate this issue. In Figure 8 we compare the *K*-band host and nuclear luminosities of the quasars. While the host luminosity is distributed over a range of only ∼2 mag, the nuclear luminosities span over ∼4 mag. As it is apparent from Figure 8, there is no clear correlation between the two quantities in our sample. The application of the Spearman rank correlation test yields no correlation ($R_S = 0.42$) with a probability of chance correlation $p = 10\%$. A similar negative result was also obtained from the study of lower redshift quasars by Dunlop et al. (2003) and Pagani et al. (2003). If we supplement our host-galaxy and nuclear data set with those from Kukula et al. (2001) and Ridgway et al. (2001), we find a modest correlation ($R_S = 0.53$, $p \sim 3\%$). However, note that

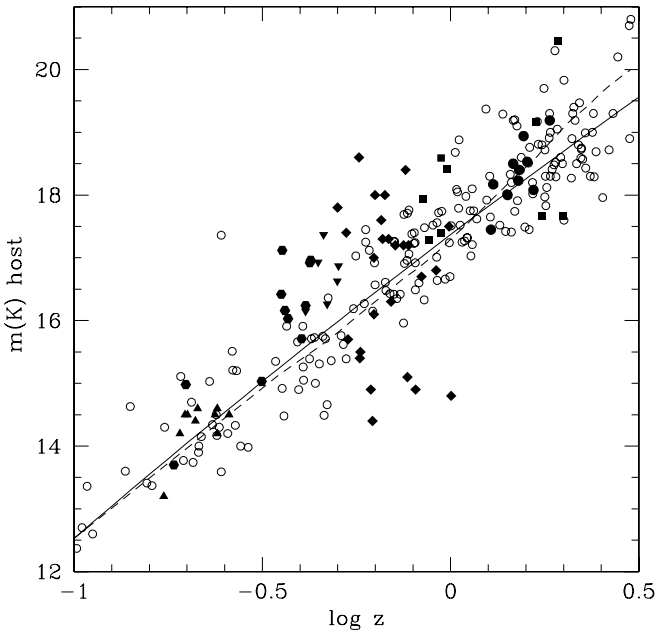

FIG. 7.—*K*-band apparent magnitude of the host galaxies vs. the redshift for RLQ samples at high redshift (*filled circles*, this work; *filled squares*, Kukula et al. 2001), intermediate-redshift objects (*filled diamonds*, Kotilainen et al. 1998 and Kotilainen & Falomo 2000; *filled inverted triangles*, Hooper et al. 1997), and low redshift (*filled hexagons*, Pagani et al. 2003; *filled triangles*, Dunlop et al. 2003). Also shown are data for RGs (*open circles*, Willott et al. 2003), the best-fit relationship for RGs (*solid line*, Willott et al. 2003) and the model of passive evolution (*dashed line*, Bressan et al. 1998).

the distribution of nuclear and host luminosities is different for RLQs and RQQs. If the two subsamples are considered separately, again no significant correlation is found between the nuclear and host luminosities ($R_S \approx 0.3$, $p \sim 30\%$). Some positive correlation was previously reported for lower redshift quasars by Hooper et al. (1997). Also in this case, however, the alleged correlation strongly depends on the fact that the RLQ and RQQ hosts have a significantly different distribution of nuclear luminosity (RQQ nuclei are $\sim$1 mag fainter than those of RLQs) and that the RQQ hosts are fainter than those of the RLQs.

Assuming that the bolometric luminosity emitted from the nucleus scales as the *K*-band luminosity (e.g., Laor & Draine 1993) and that the host-galaxy luminosity is proportional to the BH mass, it turns out that the ratio $\eta = L_{\rm nuc}/L_{\rm host}$ is proportional to the Eddington factor $\xi = L/L_E$, where $L_E = 1.25 \times 10^{38}(M_{\rm BH}/M_\odot)$. In Figure 9 we report the distribution of the *K*-band nucleus-to-host luminosity ratio. The average values for our full sample of 16 quasars is $\langle \log (M_{\rm nuc}/M_{\rm host}\rangle_{\rm All} = 1.35 \pm 0.34$. If RLQs and RQQs are considered separately an indistinguishable value is obtained: $\langle \log (M_{\rm nuc}/M_{\rm host})\rangle_{\rm RLQ} = 1.36 \pm 0.33$ and $\langle \log (M_{\rm nuc}/M_{\rm host})\rangle_{\rm RQQ} = 1.32 \pm 0.37$. On average our observed objects have a larger ratio nucleus/host with respect to the other quasars (Kukula et al. 2001; Ridgway et al. 2001) in the redshift range $z = 1$–2 discussed in this work (see Fig. 9).

Our results (see Figs. 8 and 9) therefore indicate that for high-redshift quasars, ξ is not constant, but varies in a range of $\Delta\xi \approx 1.5$ dex. There is no significant difference in $\Delta\xi$ between RLQs and RQQs. A similar spread in ξ was found for low-redshift ($z < 0.5$) RLQs (Pagani et al. 2003), suggesting that $\Delta\xi$ does not significantly depend on the redshift. This works against an interpretation of the cosmological evolution of quasars as being purely due to a strong luminosity evolution and is more consistent with a density evolution of BH activity due to increased merger and fueling rate at high redshift. The same conclusion was reached by Kukula et al. (2001) on the basis of the observed modest evolution of quasar hosts (and their central BHs) from $z = 2$ to the present epoch.

6. SUMMARY AND CONCLUSIONS

We have presented homogeneous high-quality NIR images for a sample of 17 quasars in the redshift range $1 < z < 2$. The observations, obtained under excellent seeing conditions, allowed us to characterize the properties of the quasar host galaxies and to make a reliable comparison between RLQ and RQQ hosts at high redshift.

Quasar host galaxies appear to follow the same trend in luminosity of massive inactive ellipticals that are undergoing simple passive evolution. There is no significant drop in the host mass (at least until redshift $z \sim 2$) as would be (naively) expected in the models of joint formation and evolution of galaxies and active nuclei based on the hierarchical structure formation scenario. If this drop of mass (luminosity) occurs, it must take place at epochs earlier than $z = 2$. The same increase of host-galaxy luminosity with redshift is observed both for RLQs and RQQs, suggesting that in spite of their different radio properties, the two types of quasars are hosted by galaxies that follow the same kind of evolution. However, a systematic difference in luminosity (and therefore likely in

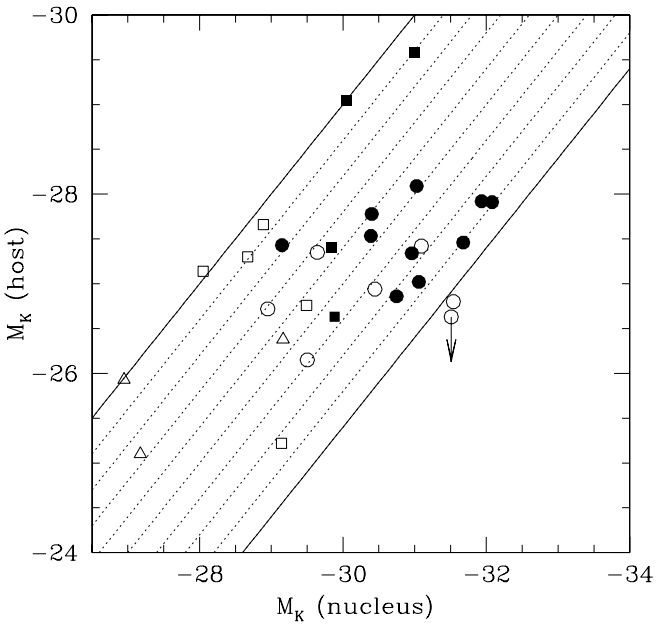

FIG. 8.—Absolute magnitude of the nucleus compared with that of the host galaxy. RLQs (*filled circles*) and RQQs (*open circles*) spanning a similar range of nuclear luminosity are hosted in galaxy of $\sim$1 mag difference, while nuclear luminosity ranges about 3 mag. The arrow represents the upper limit of the host luminosity derived for the unresolved object HE 0935−1001. No significant correlation is found. For comparison, data from Kukula et al. (2001; *squares*) and Ridgway et al. (2001; *triangles*) are also reported. Diagonal lines represent the loci of constant ratio between host and nuclear emission. These can be translated into Eddington ratios assuming that the central BH mass–galaxy luminosity correlation holds up to $z \sim 2$ and that the observed nuclear power is proportional to the bolometric emission. Separations between dotted lines correspond to a difference by a factor of 2 in the nucleus-to-host luminosity ratio. The two solid lines encompass a spread of 1.5 dex in this ratio.

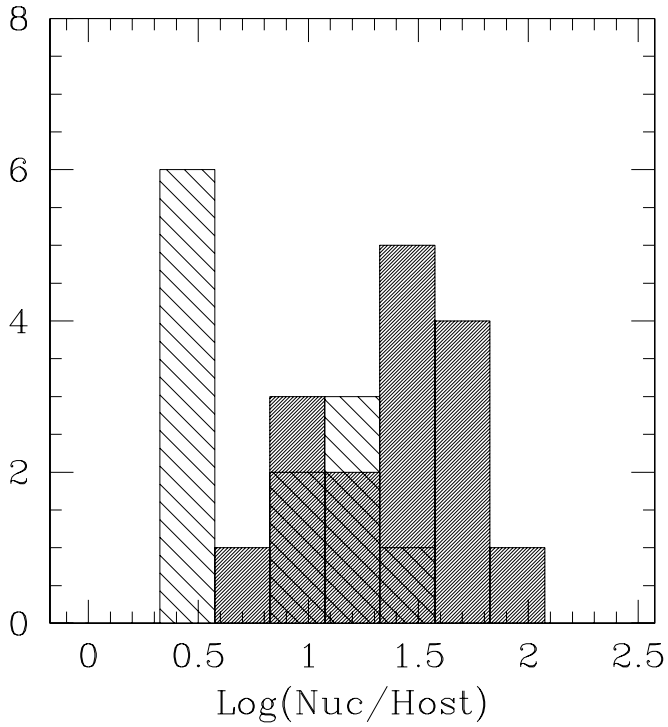

FIG. 9.—Distribution of the nuclear-to-host luminosity ratio η for the whole sample of high-redshift quasars observed at VLT (*shaded area*) compared with that of the 12 objects studied by Kukula et al. (2001) and Ridgway et al. (2001). Our sample show on average an higher nuclear-to-host luminosity ratio [$\langle \log (\mathrm{nuc}/\mathrm{host}) \rangle = 1.3$] with respect to the other quasars considered in this study [$\langle \log (\mathrm{nuc}/\mathrm{host}) \rangle = 0.8$]qq. For the VLT sample no significant difference of nucleus/host ratio is found between RLQs and RQQs, which also exhibit a similar spread ($\sim$1.5 dex) of the nucleus/host ratio.

mass) is well apparent, indicating that RLQ hosts are on average a factor of $\sim$2 more luminous (massive) than RQQ hosts, a difference that does not appear to change significantly with the redshift. This result appears robust since the comparison is based on samples with the same redshift distribution and similar nuclear luminosities. Nevertheless, we note that the size of the available samples of reliable quasar host detection at high redshift is still rather small, and the objects do not cover the luminosity-redshift plane with adequate sampling. Consequently, larger samples, possibly covering homogeneously the full range of nuclear luminosity over a wide redshift interval, are required to properly investigate whether and how the nuclear luminosity contributes to the luminosity gap between RLQ and RQQ hosts. In this regard we also remark the intriguing recent result reported by Floyd et al. (2004), who found no difference (on average) between the host luminosity of RLQ and RQQ for a sample of 17 quasars at $z \sim 0.4$ investigated using *HST* images.

The ratio between nuclear and host-galaxy luminosities for the high-redshift quasars exhibits a spread of $\sim$1.5 dex. If the host-galaxy luminosities are directly proportional to the BH mass, the observed spread indicates that the quasars radiate with a wide range of power with respect to their Eddington luminosity. The data presented here compared with the results of low-redshift sources indicate that this spread does not depend on the redshift or on the radio properties of the quasars.

Since the peak epoch of quasar activity occurs at $z \sim 2.5$, it will be of great importance to understand whether this trend exhibited by the quasar hosts is also followed by even higher redshift quasars. Exploring this issue requires the reliable characterization of the hosts of very distant quasars and therefore has to use facilities capable of high sensitivity and very narrow PSF to reduce the contribution from the nucleus to the extended emission. We have started a program to tackle this problem using VLT and NIR adaptive optics imaging with NACO (Lagrange et al. 2003).

We thank M. Kukula and S. Ridgway for providing useful information about the treatment of their published data. We also thank the anonymous referee for constructive comments and suggestions that improved the presentation of the results of this article. This work was partially supported by the Italian Ministry for University and Research (MIUR) under COFIN 2002/27145, ASI-IR 115, ASI-IR 35, and ASI-IR 73 and by the Academy of Finland (project 8201017). This publication makes use of data products from the Two Micron All Sky Survey, which is a joint project of the University of Massachusetts and the Infrared Processing and Analysis Center/California Institute of Technology, funded by the National Aeronautics and Space Administration and the National Science Foundation. This research has made use of the NASA/IPAC Extragalactic Database (NED), which is operated by the Jet Propulsion Laboratory, California Institute of Technology, under contract with the National Aeronautics and Space Administration.

REFERENCES

Abraham, R. G., Crawford, C. S., & McHardy, I. M. 1992, ApJ, 401, 474
Abraham, R. G., van den Bergh, S., Glazebrook, K., Ellis, R. S., Santiago, B. X., Surma, P., & Griffiths, R. E. 1996, ApJS, 107, 1
Aretxaga, I., Terlevich, R. J., & Boyle, B. J. 1998, MNRAS, 296, 643
Bahcall, J. N., Kirhakos, S., Saxe, D. H., & Schneider, D. P. 1997, ApJ, 479, 642
Best, P. N., Longair, M. S., & Röttgering, H. J. A. 1998, MNRAS, 295, 549
Boyce, P. J., Disney, M. J., Blades, J. C., Boksenberg, A., Crane, P., Deharveng, J. M., Macchetto, F. D., Mackay, C. D., & Sparks, W. B. 1998, MNRAS, 298, 121
Boyle, B. J. 2001, Advanced Lectures on the Starburst-AGN Connection, ed. I. Aretxaga, D. Kunth, R. Mujica (Singapore: World Scientific), 325
Boyle, B. J., & Terlevich, R. J. 1998, MNRAS, 293, L49
Bressan, A., Granato, G. L., & Silva, L. 1998, A&A, 332, 135
Canalizo, G., & Stockton, A. 2000, ApJ, 528, 201
Cimatti, A. 2003, Ap&SS, 285, 231
Cuby, J. G., Lidman, C., Moutou, C., & Petr, M. 2000, Proc. SPIE, 4008, 1036
Devillard, N. 1999, in ASP Conf. Ser. 172, Astronomical Data Analysis Software and Systems VIII, ed. D. M. Mehringer, R. L. Plante, & D. A. Roberts (San Francisco: ASP), 333
de Vries, W. H., O'Dea, C. P., Barthel, P. D., Fanti, C., Fanti, R., & Lehnert, M. D. 2000, AJ, 120, 2300
Disney, M. J., et al. 1995, Nature, 376, 150
Dunlop, J. S., McLure, R. J., Kukula, M. J., Baum, S. A., O'Dea C. P., & Hughes, D. H. 2003, MNRAS, 340, 1095
Dunlop, J. S., & Peacock, J. A. 1990, MNRAS, 247, 19
Falomo, R., Carangelo, N., & Treves, A. 2003, MNRAS, 343, 505
Falomo, R., Kotilainen, J. K., & Treves, A. 2001, ApJ, 547, 124 (FKT01)
Ferrarese, L. 2002, Proc. Second KIAS Astrophysics Workshop, ed. C.-H. Lee & H.-Y. Chang (Singapore: World Scientific), 3
Floyd, D. J. E., Kukula, M. J., Dunlop, J. S., McClure, R. J., Miller, L., Percival, W. J., Baum, S. A., & O'Dea, C. P. 2004, MNRAS, in press (astro-ph/0308436)
Franceschini, A., Hasinger, G., Miyaji, T., & Malquori, D. 1999, MNRAS, 310, L5

Francis, P. J. Whiting, M. T., & Webster, R. L. 2000, Publ. Astron. Soc. Australia, 17, 56
Hamilton, T. S., Casertano, S., & Turnshek, D. A. 2002, ApJ, 576, 61
Heckman, T. M., Miley, G. K., Lehnert, M. D., & van Breugel, W. 1991, ApJ, 381, 373
Hooper, E. J., Impey, C. D., & Foltz, C. B. 1997, ApJ, 480, L95
Hutchings, J. B. 1998, AJ, 116, 20
Hutchings, J. B., Crampton, D., & Campbell, B. 1984, ApJ, 280, 41
Hutchings, J. B., Crampton, D., Morris, S. L., Durand, D., & Steinbring, E. 1999, AJ, 117, 1109
Kauffmann, G., & Haehnelt, M. 2000, MNRAS, 311, 576
Kauffmann, G., et al. 2003, MNRAS, 341, 54
Kinney, A. L., Calzetti, D., Bohlin, R. C., McQuade, K., Storchi-Bergmann, T., & Schmitt, H. R. 1996, ApJ, 467, 38
Kirhakos, S., Bahcall, J. N., Schneider, D. P., & Kristian, J. 1999, ApJ, 520, 67
Koo, D. C., et al. 1996, ApJ, 469, 535
Kormendy, J., & Gebhardt, K. 2001, in AIP Conf. Proc. 586, 20th Texas Symp. Relativistic Astrophysics, ed. J. C. Wheeler & H. Martel (Melville: AIP), 363
Kormendy, J., & Richstone, D. 1995, ARA&A, 33, 581
Kotilainen, J. K., & Falomo, R. 2000, A&A, 364, 70
Kotilainen, J. K., Falomo, R., & Scarpa, R. 1998, A&A, 332, 503
Kukula, M. J., Dunlop, J. S., McLure, R. J., Miller, L., Percival, W. J., Baum, S. A., & O'Dea, C. P. 2001, MNRAS, 326, 1533
Lacy, M., Bunker, A. J., & Ridgway, S. E. 2000, AJ, 120, 68
Lagrange, A.-M., et al. 2003, Proc. SPIE, 4841, 860
Laor, A., & Draine, B. T. 1993, ApJ, 402, 441
Le Fevre, O., et al. 2000, MNRAS, 311, 565
Lehnert, M. D., Heckman, T. M., Chambers, K. C., & Miley, G. K. 1992, ApJ, 393, 68
Lehnert, M. D., van Breugel, W. J. M., Heckman, T. M., & Miley, G. K. 1999, ApJS, 124, 11
Lowenthal, J. D., Heckman, T. M., Lehnert, M. D., & Elias, J. H. 1995, ApJ, 439, 588
Madau, P., Pozzetti, L., & Dickinson, M. 1998, ApJ, 498, 106
Magorrian, J., et al. 1998, AJ, 115, 2285
McLeod, K. K., & Rieke, G. H. 1994, ApJ, 431, 137
Mobasher, B., Sharples, R. M., & Ellis, R. S. 1993, MNRAS, 263, 560
Nolan, L. A, Dunlop, J. S., Kukula, M. J., Hughes, D. H., Boroson, T, & Jimenez, R. 2001, MNRAS, 323, 308
Pagani, C., Falomo, R., & Treves, A. 2003, ApJ, 596, 830
Pentericci, L., McCarthy, P. J., Röttgering, H. J. A., Miley, G. K., van Breugel, W. J. M., & Fosbury, R. 2001, ApJS, 135, 63
Percival, W. J., Miller, L., McLure, R. J., & Dunlop, J. S. 2001, MNRAS, 322, 843
Poggianti, B. M. 1997, A&AS, 122, 399
Ridgway, S., Heckman, T., Calzetti, D., & Lehnert, M. 2001, ApJ, 550, 122
Smith, E. P. Heckman, T. M. Bothun, G. D., Romanishin, W., & Balick, B. 1986, ApJ, 306, 64
Steidel, C. C., Adelberger, K. L., Giavalisco, M., Dickinson, M., & Pettini, M. 1999, ApJ, 519, 1
Taylor, G. L., Dunlop, J. S., Hughes, D. H., & Robson, E. I. 1996, MNRAS, 283, 930
Veron-Cetty, M. P., & Veron, P. 2001, A&A, 374, 92
Veron-Cetty, M. P., & Woltjer, L. 1990, A&A, 236, 69
Warren, S. J., Hewett, P. C., & Osmer, P. S. 1994, ApJ, 421, 412
Willott, C. J., Rawlings, S., Jarvis, M. J., & Blundell. K. M. 2003, MNRAS, 339, 173
Zirm, A. W., Dikinson, M., & Dey, A. 2003, ApJ, 585, 90